

Research on a Method for the Optical Measurement of the Rifling Angle of Artillery Based on Angle Error Correction

Ye Zhang and Yang Zheng*

*Changchun University of Science and Technology, School of Opto-Electronic Engineering,
Changchun 130022, China*

(Received July 22, 2020 : revised September 14, 2020 : accepted September 28, 2020)

The rifling angle of artillery is an important parameter, and its determination plays a key role in the stability, hit rate, accuracy and service life of artillery. In this study, we propose an optical measurement method for the rifling angle based on angle error correction. The method is based on the principle of geometrical optics imaging, where the rifling on the inner wall of the artillery barrel is imaged on a CCD camera target surface by an optical system. When the measurement system moves in the barrel, the rifling image rotates accordingly. According to the relationship between the rotation angle of the rifling image and the travel distance of the measurement system, different types of rifling equations are established. Solving equations of the rifling angle are deduced according to the definition of the rifling angle. Furthermore, we added an angle error correction function to the method that is based on the theory of dynamic optics. This function can measure and correct the angle error caused by the posture change of the measurement system. Thus, the rifling angle measurement accuracy is effectively improved. Finally, we simulated and analyzed the influence of parameter changes of the measurement system on rifling angle measurement accuracy. The simulation results show that the rifling angle measurement method has high measurement accuracy, and the method can be applied to different types of rifling angle measurements. The method provides the theoretical basis for the development of a high-precision rifling measurement system in the future.

Keywords : Optical measurement, Rifling angle, Angle error correction, Geometric optics

OCIS codes : (080.0080) Geometric optics; (110.0110) Imaging systems; (120.4290) Nondestructive testing; (120.4640) Optical instruments

I. INTRODUCTION

The barrel is the most important part of artillery, and rifling is the soul of the barrel. Rifling refers to the spiral grooves in the inner wall of the artillery barrel. Its function is to send the projectile into the air at a certain rotation speed to maintain stability. The angle between the tangent line at a point on the rifling and the barrel axis is called the rifling angle [1]. The rifling angle is an important parameter of artillery, and has a great influence on its stability, hit rate, strike accuracy and service life. According to the distinct rifling angle, rifling can be divided into rib rifling and increasing rifling. The rifling

angle of rib rifling is constant, while the rifling angle of increasing rifling is increasing [2].

Due to the long length and small diameter of the barrel, it is still difficult to accurately measure the rifling angle. Rifling angle measurement methods are mainly divided into two categories: contact measurement methods and optical measurement methods. The typical contact measurement methods are the air plug rail method and stylus method. The measuring instruments for these methods are in direct contact with the rifling to obtain the rifling profile, and then calculate the rifling angle according to the rifling profile. These methods can calculate the size of the rifling angle qualitatively, but not quantitatively [3]. Also, it is

*Corresponding author: 747421565@qq.com, ORCID 0000-0003-2407-9887

Color versions of one or more of the figures in this paper are available online.



This is an Open Access article distributed under the terms of the Creative Commons Attribution Non-Commercial License (<http://creativecommons.org/licenses/by-nc/4.0/>) which permits unrestricted non-commercial use, distribution, and reproduction in any medium, provided the original work is properly cited.

easy to damage the rifling with the contact measurement methods. Therefore, all kinds of optical measurement methods for the rifling angle have become mainstream in recent years. Typical optical measurement methods include the optical single-point scanning method, laser triangulation method and light projection method [4]. The optical single-point scanning method and laser triangulation method use an instrument to scan the barrel's inner wall to obtain the rifling profile and further calculate the rifling angle. These methods can only scan rifling sections one by one, which makes their measurement efficiency very low. The light projection method can be used to image the rifling on the inner wall of the barrel, and the rifling angle can be further calculated according to the information of the rifling image. The light projection method has high measurement efficiency and is widely used. J. Zheng *et al.* [4] has proposed a method based on image conversion to obtain the rifling image, and further calculated the parameters of rifling [5-7]. J. Wang *et al.* [8] proposed to use an image processing method to calculate the rifling angle by combining the rifling equation and the rifling boundary conditions, but due to the influence of the image quality and light conditions, the measurement accuracy of the method is low [8]. H. Ma *et al.* [9] used optical triangulation technology to obtain a rifling contour image from the inner wall of the barrel, and obtained the related information of rifling parameters from the rifling image based on image processing technology [9]. Z.-W. Feng *et al.* [10] put forward a kind of rifling angle measurement technology based on the template matching method, which realizes the measurement of the rifling angle of multiple types of rifling [10]. Toivola *et al.* [11] and Keinänen *et al.* [12] used finite element analysis to explore the correlation measurement. J. Sun *et al.* [13] analyzed the influence of the rifling on the rotating belt of a shell, and studied the motion law of the rotating belt in the transition section of compound rifling and the relevant parameters of rifling [13].

In this paper, an optical measurement method for the rifling angle of artillery is proposed. The method derives the rifling angle solving equations according to the relation-

ship between object and image in geometrical optics. Moreover, the method has an angle error correction function, which can effectively improve the accuracy of rifling angle measurement.

II. PRINCIPLE OF RIFLING ANGLE MEASUREMENT BASED ON OPTICAL IMAGING

As shown in Fig. 1, a light source illuminates the inner wall of the barrel, and the rifling is imaged by the optical system on the CCD camera target surface. There are two points on the barrel inner wall, M_1 and M_0 , and their image points M'_1 and M'_0 are obtained by the axicon mirror's reflection. Point M_1 is just reflected by the edge of the axicon mirror, and point M_0 is reflected by the tip of the axicon mirror. So, the measurement range of the measurement system is an annular area from point M_0 to point M_1 . Point M is located between point M_1 and point M_0 , and its image reflected by the axicon mirror is point M' . The plane where points M'_0 , M'_1 and M' are located is the image plane of points M_0 , M_1 and M . The inclination angle of the reflecting surface of the axicon mirror is 45° , so the distance from the image plane to the tip of the axicon mirror is R (the barrel radius). When the optical system images the barrel inner wall, the image plane is equivalent to an object plane, so the points M'_0 , M'_1 and M' are imaged on the CCD camera target surface by the optical system, and the images are the points M''_0 , M''_1 and M'' , which lie in the circle with radius r [8].

The initial position of the rifling angle measurement system is set at the head of the barrel. A rectangular coordinate system is established by taking the intersection point of the CCD camera target surface and the barrel axis as the origin, and the barrel axis is the z axis. The distance between the center point of the optical system and the tip of the axicon mirror is a , and the distance between the optical system center point and the CCD camera target surface is l [6].

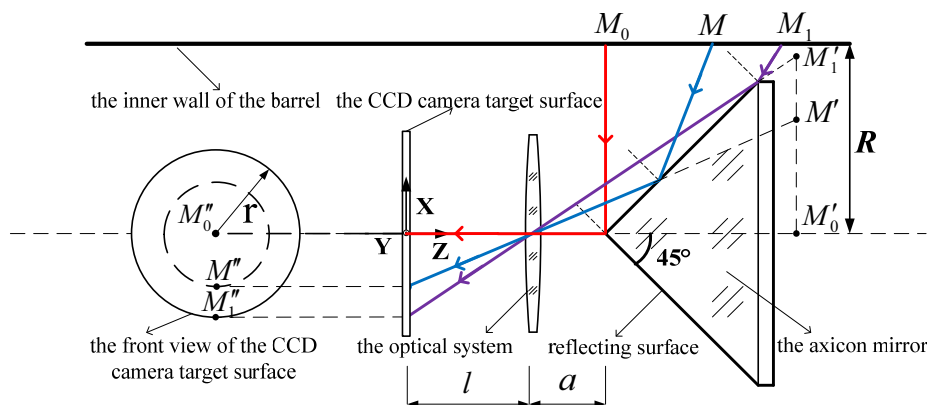


FIG. 1. Optical schematic diagram of rifling imaging.

Suppose the rectangular coordinates of point M are (x, y, z) , and its cylindrical coordinates are (ρ, ϕ, z) . The polar diameter ρ of point M in the cylindrical coordinates is equal to the barrel radius R . Therefore, the relationships between the cylindrical coordinates and rectangular coordinates of point M are

$$\begin{cases} x = R \cos \phi \\ y = R \sin \phi \\ z = z, \end{cases} \quad (1)$$

where ϕ is the polar angle of point M in the cylindrical coordinate system, and z is the z-axis coordinate of point M in the cylindrical coordinate system.

The inclination angle of the reflecting surface of the axicon mirror is 45° , and the coordinates of point M' are

$$\begin{cases} \rho' = z - a - l \\ \phi' = \phi \\ z' = l + a + R, \end{cases} \quad (2)$$

where ρ' , ϕ' and z' are the polar diameter, polar angle and z-axis coordinate of point M' , respectively, in the cylindrical coordinate system.

According to the magnification relation of object and image in geometrical optics, the coordinate of point M'' is

$$\begin{cases} \rho'' = (l - f)(z - a - l) / f \\ \phi'' = \phi \\ z'' = 0, \end{cases} \quad (3)$$

where f is the focal length of the optical system, and ρ'' , ϕ'' and z'' are the polar diameter, polar angle and z-axis coordinate of point M'' , respectively, in the cylindrical coordinate system.

An image of rib rifling on the CCD camera target surface made by the measurement system is shown in Fig. 2.

When the measurement system moves along the axis in the barrel, the rifling image on the CCD camera target surface rotates accordingly. As shown in Fig. 2, N_1 is the

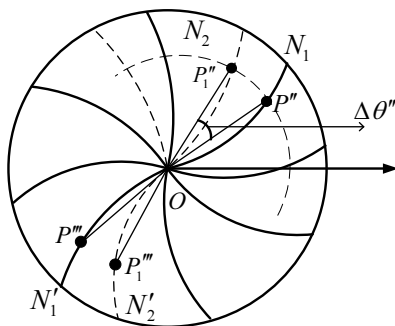


FIG. 2. Schematic diagram of rib rifling image on the CCD camera target surface.

initial position of a certain rifling image, and N_2 is the position of N_1 after the forward movement distance Δz of the measurement system in the barrel. Point P'' is marked on N_1 , and point P_1'' is marked on N_2 . Points P'' and P_1'' have the same ρ'' value on the CCD camera target surface. $\Delta\theta''$ is the angle between points P'' and P_1'' , which can be measured by the CCD camera's external calculator. When the measurement system is eccentric in the barrel, the center point of the rifling image is not in the center of the target surface, so the measurement result of angle $\Delta\theta''$ has an error. Suppose the center point of the target surface is O , then N_1' and N_2' are the symmetrical rifling of N_1 and N_2 , as shown in Fig. 2. Points P''' and P_1''' on N_1' and N_2' are marked with the same curvature as point P'' . So, the intersection point of line $P''P'''$ and line $P_1''P_1'''$ is the rifling image center point O_1 . Point O_1 and point O are overlapped by the image processing technology, so the measurement result of angle $\Delta\theta''$ is not affected by the eccentricity of the measurement system. The corresponding object points of points P'' and P_1'' on the rifling are P and P_1 , and $\Delta\theta$ is the angle between point P and points P_1 on the barrel circumference relative to the barrel axis, so it can be concluded from Eq. (3) that $\Delta\theta = \Delta\theta''$. The arc length from point P to point P_1 on the circumference of the barrel is $\Delta\theta \cdot R$ (where $\Delta\theta$ is a radian number).

For the rib rifling, because it's rifling angle is constant, if the barrel is expanded into a plane, rib rifling is an inclined straight line, as shown in Fig. 3. The relationship between the arc length from P to P_1 on the circumference of the barrel and the travel distance of the measurement system can be expressed as a linear function:

$$\Delta\theta \cdot R = k \cdot \Delta z. \quad (4)$$

The rib rifling equation is as follows:

$$\theta R = kz + C, \quad (5)$$

where k is the rifling equation coefficient, C is the constant, z is the axial measurement distance of the measurement system and θ is the rotation angle of the measurement point on the rifling relative to the initial position.

According to the definition of the rifling angle

$$\tan \alpha = \frac{d\theta}{dz} R, \quad (6)$$

where α is the rifling angle.

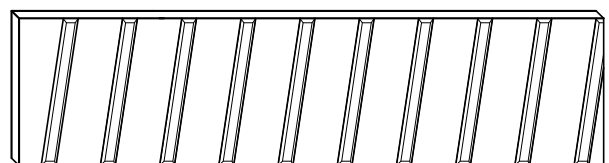


FIG. 3. Panorama of the rib rifling.

Introducing Eq. (5) in Eq. (6), the rifling angle of the rib rifling can be obtained as follows:

$$\alpha = \arctan k. \tag{7}$$

When the measurement system moves in the barrel, it will rotate due to vibration and other factors. When the measurement system rotates, there will be an error in the rifling angle measurement results, which is called angle error. In order to improve rifling angle measurement accuracy, an angle error correction function based on the theory of dynamic optics was added to the measurement system.

The angle error correction function uses the reflection characteristics of a right-angle prism to measure the angle error. The measurement principle is shown in Fig. 4 [14]. When the measurement system is in the initial position, the ridge of the right-angle prism is placed horizontally, and when the measurement system rotates, the right-angle prism will rotate at the same angle. The crosshairs on a reticle outside the measurement system are imaged on the CCD camera target surface by the right-angle prism, and the rotation of the measurement system will cause the image of the crosshairs to rotate accordingly. Suppose the rotation angle of the measurement system is φ , and the corresponding rotation angle of the crosshair image is γ . The measurement of the angle error is completed according to the relationship between them.

The relationship between angle φ and angle γ is deduced as follows. As shown in Fig. 4, the object coordinates system $Oxyz$ and the image coordinates system $O'x'y'z'$ are established. When the rotation angle of the right-angle

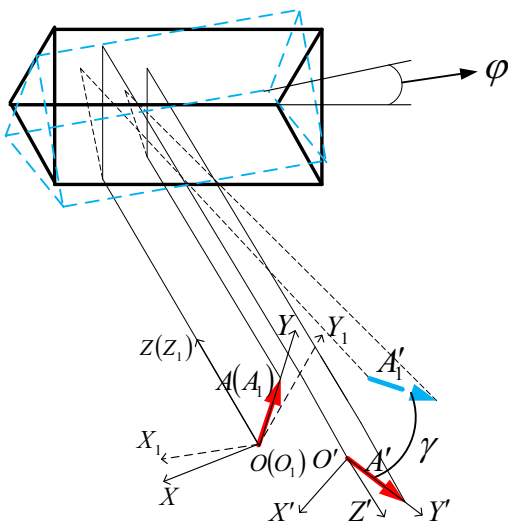


FIG. 4. Schematic diagram of the rotation angle of the crosshair image caused by the rotation of the right-angle prism. A is the crosshair object vector without rotation, A' is the crosshair image vector without rotation, A_i is the crosshair object vector after rotation, and A'_i is the crosshair image vector after rotation.

prism around the incident optical axis z is φ , the object coordinates system $Oxyz$ is changed into $O_ix_iz_i$.

According to the theory of dynamic optics [15], the base coordinates of A and A' in their respective coordinate systems are (i, j, k) and (i', j', k') , the conversion relationship between them is $(i', j', k') = (i, j, k)R_0$. And R_0 is the base transformation matrix from the object coordinates to the image coordinates, and it can be expressed as

$$R_0 = \begin{pmatrix} \cos(x, x') & \cos(x, y') & \cos(x, z') \\ \cos(y, x') & \cos(y, y') & \cos(y, z') \\ \cos(z, x') & \cos(z, y') & \cos(z, z') \end{pmatrix}. \tag{8}$$

The magnification of the right-angle prism to the object is 1, therefore, the right-angle prism magnification matrix is $B = E$. When the right-angle prism does not rotate, $A' = BRA$, and $R = BR_0$, R is the action matrix of the right-angle prism [16, 17]:

$$R = \begin{pmatrix} 1 & 0 & 0 \\ 0 & -1 & 0 \\ 0 & 0 & -1 \end{pmatrix}. \tag{9}$$

When the right-angle prism rotation angle is φ , A changes into A_i , and $A_i = SA$. S is the rotation matrix, and it can be expressed as

$$S = \begin{pmatrix} \cos \varphi & \sin \varphi & 0 \\ -\sin \varphi & \cos \varphi & 0 \\ 0 & 0 & 1 \end{pmatrix}. \tag{10}$$

After the right-angle prism rotates, the mathematical relationship between A'_i and A is $A'_i = SRS^{-1}A$. Suppose A is $[0, 1, 0]^T$, and A'_i is $[-\sin 2\varphi, -\cos 2\varphi, 0]^T$ after being reflected by the right-angle prism. As shown in Fig. 5, according to the position of A' and A'_i on the CCD camera target surface, the relationship between φ and γ is

$$\tan \gamma = \frac{-\sin 2\varphi}{-\cos 2\varphi} \Rightarrow \gamma = 2\varphi. \tag{11}$$

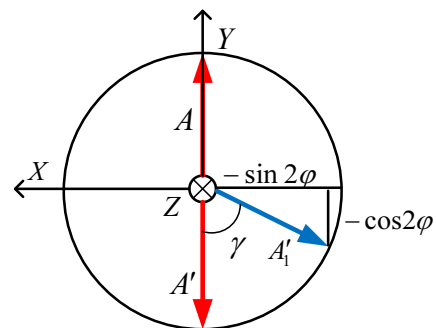


FIG. 5. Schematic diagram of the object vector and image vector on the CCD camera target surface.

After the angle error is measured, the actual rotation angle between point P and point P_1 is $\Delta\theta_1 = \Delta\theta + \varphi$. When the rotation angle of the measurement system is the same as that of the rifling image, φ is positive; otherwise, φ is negative. By substituting $\Delta\theta_1$ and Δz into Eq. (4), the exact value of k can be obtained according to the over positive definite equation, and Δz can be measured by the laser rangefinder in the measurement system.

For the increasing rifling, the rifling equation is a non-linear curve, which is assumed to be a conic [10]. When the travel distance of the measurement system is short, the rifling equation from point P to point P_1 can still be expressed by Eq. (5). Assuming the barrel length is Z , the conic increasing rifling equation is as follows:

$$\theta(\text{rad})R = \int_0^Z (kz + C)dz = k_1 z^2 + k_2 z + C. \quad (12)$$

Similarly, k_1 and k_2 can be calculated according to the over positive definite equation. According to Eq. (6), the rifling angle solving equation of the conic increasing rifling is

$$\alpha = \arctan(2k_1 z + k_2). \quad (13)$$

Substituting Eq. (3) into Eq. (13), the rifling angle solving equation of point M is

$$\alpha = \arctan \left[2k_1 \left((\rho'' + l) \frac{f}{l-f} + l - R \right) + k_2 \right]. \quad (14)$$

When the travel distance of the measurement system is Δz , the ρ'' value of point M changes to $\rho'' + \Delta\rho$. It can be known from Eq. (3) that $\Delta\rho = \Delta z(l-f)/f$. Therefore, the rifling angle solving equation at any point on the CCD camera target surface is

$$\alpha = \arctan \left[2k_1 \left((\rho'' + l + \Delta\rho) \frac{f}{l-f} + l - R \right) + k_2 \right]. \quad (15)$$

Eq. (7) and Eq. (15) are the rifling angle solving equations of the rib rifling and conic increasing rifling, respectively. For the determined measurement system and the barrel to be measured, the parameters R , f and l are fixed values.

III. MEASUREMENT SYSTEM

Based on the proposed rifling angle measurement method, a measurement system with an angle error correction function was designed as shown in Fig. 6. The system consists of two parts: a rifling angle measurement device (I, III) and an angle error measurement device II.

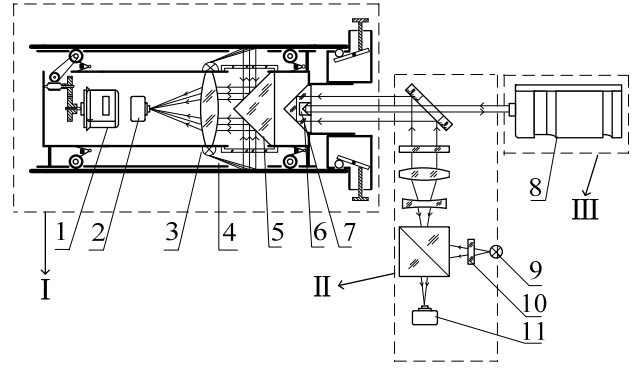


FIG. 6. Schematic diagram of the rifling angle measurement system. 1: stepping motor, 2: CCD camera I, 3: light source I, 4: sleeve, 5: axicon mirror, 6: right-angle prism, 7: angle mirror, 8: laser rangefinder, 9: light source II, 10: reticle, and 11: CCD camera II.

The stepping motor drives measurement device I to move in the barrel, and light source I illuminates the inner wall of the barrel so that the rifling is imaged on the target surface of CCD camera I by the optical system. After image processing, the rifling image rotation angle is extracted, and the rifling equation coefficients are solved. The travel distance of the measurement system is measured by the laser rangefinder. When the posture of the measurement system changes in the barrel, the rotation angle of the measurement system is measured by measurement device II, and then the angle error is corrected to improve the rifling angle measurement accuracy. The sleeve cover matched with the barrel size is outside the measurement system, and the distance between it and the barrel is about 2 mm, and the wheels of the traction device can leak from the hollow part of the sleeve. The sleeve can not only ensure the smooth movement of the measurement system in the barrel, but also guarantee the stability of the measurement system. Moreover, it can effectively reduce rifling angle measurement error caused by the eccentricity of the measurement system.

IV. SIMULATION ANALYSIS

The rifling angle measurement error was analyzed for a particular barrel according to the rifling angle solving equation of the rib rifling established in this paper. The barrel radius R is 60 mm, the barrel length Z is 5000 mm, the rifling angle α is $6^\circ 24''$, and the rifling type is rib rifling. The rifling angle α is an indirect measurement, which is determined by the rifling equation coefficient k , and $k = (\Delta\theta + \varphi)R/\Delta z$. Under the condition of not considering other errors, the errors introduced in calculating rifling coefficient k are shown in Table 1.

The errors are not related to each other. According to $\delta k^2 = \sum [\partial f / \partial x_i]^2 \delta k_i^2$ and the error transfer Eq. (16), the

TABLE 1. Measurement errors of the rifling equation coefficient k

Error sources	Error symbol	Error value
Laser rangefinder ranging error	δz	0.5 mm
Barrel radius measurement error	δR	0.15 mm
Angle error	$\delta\theta$	30"
Error in the correction of angle error	$\delta\varphi$	30"

error of the rifling equation coefficient δk is calculated, so that the rifling angle measurement error of the above-mentioned barrel is $\delta\alpha \approx 47''$:

$$\delta k = \left[\left(\frac{\theta R}{z^2} \right)^2 \delta z^2 + \left(\frac{R}{z} \right)^2 (\delta\varphi + \delta\theta)^2 + \left(\frac{\theta}{z} \right)^2 \delta R^2 \right]^{\frac{1}{2}}. \quad (16)$$

For conic increasing rifling, the rifling equation and the rifling angle solving equation established in this paper were simulated and analyzed by MATLAB software. The influence of barrel parameters and measurement system parameters on rifling angle change trends were also analyzed.

According to the simulation results in Fig. 7, the rifling angle increases with increased measurement distance, but the slope change rate of the rifling angle curve gradually decreases. It can be concluded that the rifling angle changes rapidly in the initial stage, and then changes gently.

As shown in Fig. 8, when the rifling equation coefficients k_1 and k_2 are constant values, the rifling rotation angle increases with increased barrel length, and the relationship between them is a quadratic function. The rifling rotation angle decreases with increases in the barrel radius, and the relationship between them is an inverse proportion function.

It can be seen from Fig. 9 that the rifling angle change trend is related to the barrel length and not to the barrel radius. The rifling angle increases with the barrel length and tends to a fixed value (the rifling angle theoretical limit value is 90°).

It can be seen from Fig. 10 that the rifling angle increases with the increase of k_1 and k_2 . When k_2 is a fixed value, the change of the rifling angle is obvious with the increase of k_1 , and it soon reaches the limit value and tends to be gentle. When k_1 is a fixed value, the rifling angle increases with the increase of k_2 , but the change is slow.

The measurement method proposed in this paper is based on the principle of optical imaging. The rifling is clearly imaged on the CCD camera target surface by the optical system. By moving the position of the relative image surface in the optical system, the measurement of the rifling of different caliber barrels can be realized. Finally, the relevant information for calculating the rifling

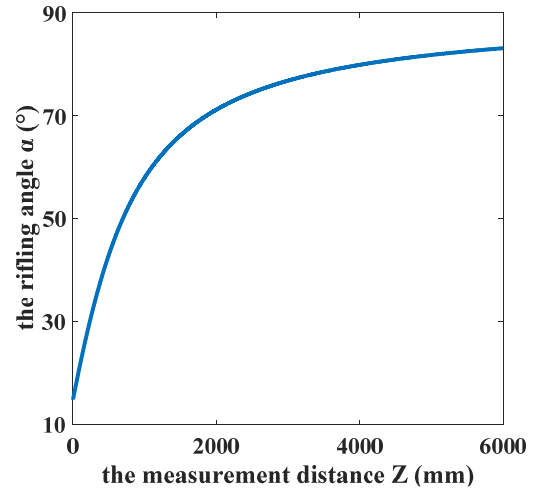


FIG. 7. Simulation curve of the rifling angle of conic increasing rifling.

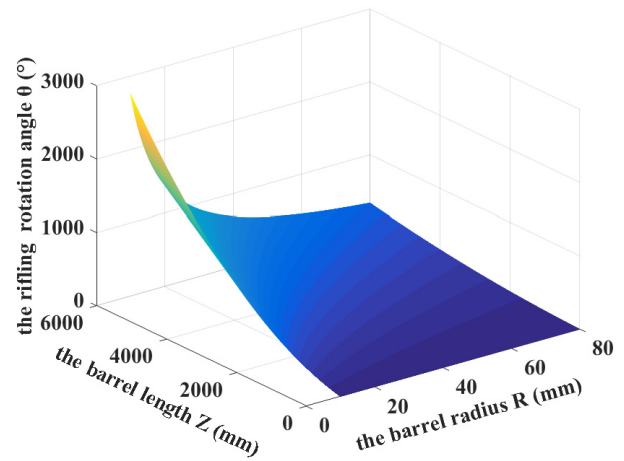


FIG. 8. Simulation diagram of the influence of barrel radius and length on the rifling rotation angle.

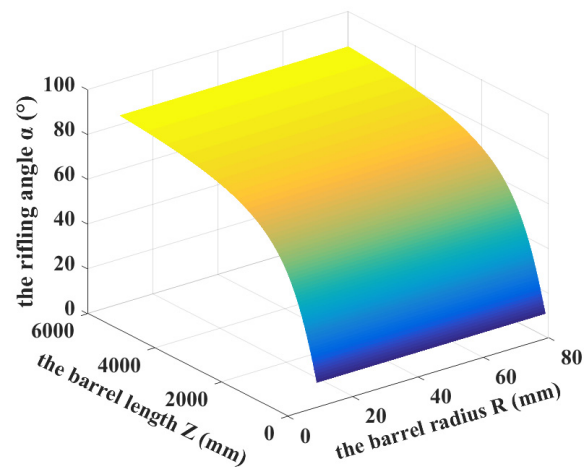


FIG. 9. Simulation diagram of the influence of barrel radius and length on the rifling angle change trend.

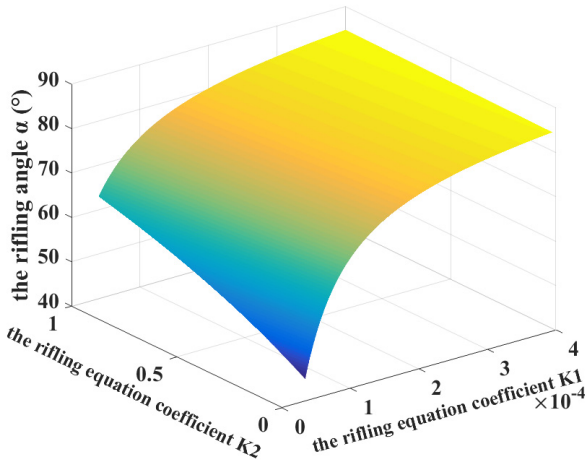


FIG. 10. Simulation diagram of the influence of the rifling equation coefficients k_1 and k_2 on the rifling angle change trend.

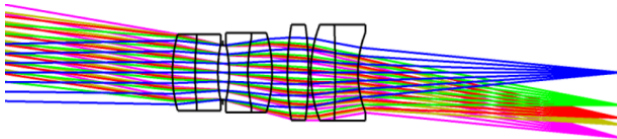


FIG. 11. Simulation diagram of the optical imaging lens of the rifling angle measurement system.

TABLE 2. Parameters values of three measurement systems

	f	l	R	a
System 1	20.000 mm	16.479 mm	60.000 mm	18.496 mm
System 2	25.000 mm	17.215 mm	60.000 mm	73.577 mm
System 3	35.000 mm	27.397 mm	60.000 mm	102.994 mm

angle can be obtained from the rifling image by the image processing technology. The lens of the optical system is shown in Fig. 11.

Focal length is a key parameter of the rifling angle measurement system, and the influence of different focal length measurement systems on measurement error are simulated and analyzed. Three measurement systems with $f = 20$ mm, $f = 25$ mm and $f = 35$ mm were designed by Zemax software and aimed at a barrel with a radius of 60 mm. The parameters of the three measurement systems are shown in Table 2.

The rifling angle measurement errors of three measurement systems were simulated by MATLAB software according to Eq. (15). Moreover, the measurement performances of the three measurement systems were also analyzed.

According to the simulation results in Fig. 12, the shorter focal length measurement system had higher measurement accuracy for the rifling angle. But the measurement results of the different focal length measurement systems were similar to each other, and with increases in the measurement

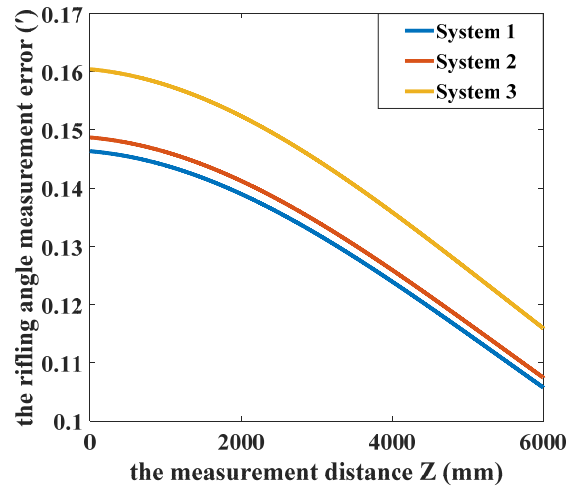


FIG. 12. Simulation curves of the rifling angle measurement errors of three measurement systems.

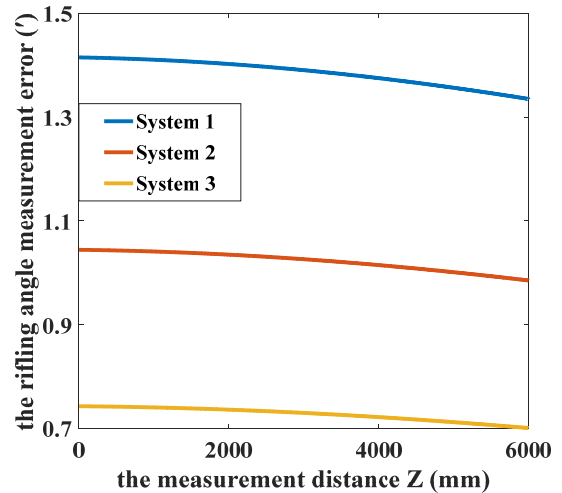


FIG. 13. Simulation curves of the influence of 0.1 mm defocusing on the rifling angle measurement errors of three measurement systems.

distance, the relative errors of the rifling angle measurement results decreased.

When the measurement system moves in the barrel, the optical system will defocus due to vibration and other factors. When defocusing occurs, the rifling imaging becomes blurred, which affects rifling angle measurement accuracy. The rifling angle measurement errors of the three measurement systems was simulated when the defocusing was 0.1 mm.

As shown in the simulation curves in Fig. 13, when the defocusing is the same, the longer focal length measurement system has higher rifling angle measurement accuracy. And with the increase of measurement distance, the rifling angle measurement error gradually decreases.

As shown with the simulation curves in Fig. 14, when the measurement accuracy is the same, the longer focal

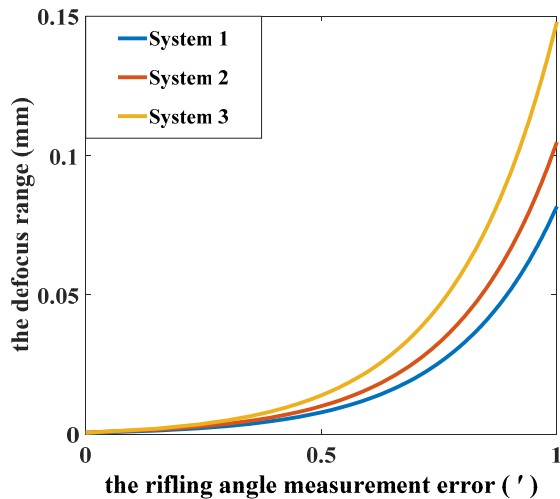


FIG. 14. Simulation curves of the defocus range of three measurement systems.

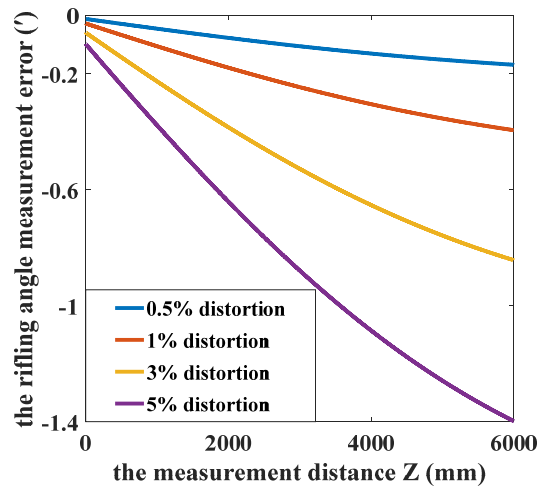


FIG. 15. Simulation curve of the rifling angle measurement error under different distortions.

length measurement system has a larger defocus range. Therefore, when the defocusing is the same, the measurement accuracy of the longer focal length measurement system is higher.

The measurement system designed in this paper can measure the rifling angle of barrels with different radiuses. The minimum working distance of a shorter focal length measurement system is smaller. Conversely, the minimum working distance of a longer focal length measurement system is larger. The above simulation results show that a shorter focal length measurement system can measure the rifling angle with higher accuracy. However, if the focal length of the measurement system is shorter, its defocusing range is also smaller. For measurement systems with $f = 20$ mm, $f = 25$ mm and $f = 35$ mm, the comprehensive analysis showed that the measurement system with $f = 25$ mm is more suitable.

When the focal length and other parameters of the measurement system are determined, the values of the rifling equation coefficients k_1 and k_2 are calculated by image processing of the rifling image. The distortion of the optical system makes the rifling image deformed, which affects the rifling angle measurement accuracy. The measurement errors of different distortions were simulated, and the imaging lens was $f = 25$ mm, field of view in angle was 23° , and $F/\#$ was 4.0. As shown in Fig. 15, as distortion increases, the rifling angle measurement error increases as well. When the rifling angle measurement accuracy is $1'$, the distortion should not exceed 3%.

V. CONCLUSION

This study proposed a rifling angle optical measurement method based on the principle of geometric optics imaging. In this method, the rifling on the inner wall of the barrel is imaged on the target surface of the CCD camera by an optical system. Rifling angle solving equations are derived according to the object-image relationship in geometric optics, and the rifling angle solving equations can be used for different types of rifling angle measurements. Moreover, based on the principle of dynamic optics, this method measures and corrects the angle error caused by vibration of the measurement system. Rifling angle measurement accuracy is effectively improved. The simulation results show that this measurement method can achieve high measurement accuracy, and the rifling angle measurement error is lower than $1'$.

ACKNOWLEDGMENT

This study was supported by the Jilin Provincial Science and Technology Department excellent young talents fund (No. 20180520201JH) and the Innovation Foundation of Changchun University of Science and Technology (No. XJLJG201806).

REFERENCES

1. H.-J. Li, W.-Q. Wang, C.-S. Li, and Y.-X. Yang, "Influence of winding angle error artillery rifling on the positioning accuracy of air-burst fuze and its compensation," *J. Beijing Inst. Technol.* **38**, 371-375 (2018).
2. Y.-F. Xu, H.-M. Ding, and J. Xu, "Numerical analysis of influence of rifling structure of large caliber gun on moving of projectile with sliding driving band in bore," *Acta Armamentarii* **37**, 2148-2156 (2016).
3. R. M. Miner, "Methods and apparatus for testing roundness and straightness of pipes and tubing," US Patent US4354379A (1982).
4. J. Zheng, C.-G. Xu, D.-G. Xiao, and Z.-S. Liu, "A compre-

- hensive measuring system for the inner surface of artillery,” *J. Beijing Inst. Technol.* **23**, 694-698 (2003).
5. J. Zheng, C.-G. Xu, and D.-G. Xiao, “New image operator and its application in the inner surface detection of artillery pipe,” *J. Beijing Inst. Technol. (Engl. Ed.)*, **12**, 307-311 (2003).
 6. J. Zheng, W. Zhang, and K.-R. Shi, “Circumferential equi-spaced curves’s image detection technique and its application on rifling angle measurement,” *Chinese J. Mech. Eng. (Engl. Ed.)*, **17**, 519-523 (2004).
 7. J. Zheng, C.-G. Xu, and D.-G. Xiao, “An image transformation technique for the detection of artillery’s rifling parameter,” *Acta Armamentarii* **25**, 134-138 (2004).
 8. J. Wang and C.-S. Shan, “New measurement system for angle of artillery,” *China Meas. Technol.* **32**, 32-34 (2006).
 9. H. Ma, Y. Che, Y. Shen, and B. Bai, “Research on opto-electronic technology for detecting rifling of artillery online,” *SPIE* **2899**, 464-469 (1996).
 10. Z.-W. Feng, K.-H. Jiao, C.-G. Xu, W.-J. Zhu, and D.-G. Xiao, “A new method for measuring the rifling angle of artillery pipe based on template matching,” *Acta Armamentarii* **29**, 1362-1366 (2008).
 11. H. Keinänen, S. Moilanen, J. Tervokoski, and J. Toivola, “Influence of rotating band construction on gun tube loading—Part I: Numerical approach,” *J. Pressure Vessel Technol.* **134**, 041006 (2012).
 12. J. Toivola, S. Moilanen, J. Tervokoski, and H. Keinänen, “Influence of rotating band construction on gun tube loading—Part II: Measurement and analysis,” *J. pressure Vessel Technology*, **134**, 041007 (2012).
 13. J. Sun, G. Chen, L. Qian, and T. Liu, “Analysis of gun barrel rifling twist,” *AIP Conf. Proc.* **1839**, 020096 (2017).
 14. P. Shi and E. Stijns, “New optical method for measuring small-angle rotations,” *Appl. Opt.* **27**, 4342-4344 (1988).
 15. S.-P. Bai, C.-Y. Wang, and C.-Y. Pang, “Study on imaging features of optic system in motion based on coordinate transformation,” *J. Appl. Opt.* **22**, 1-6 (2001).
 16. L. Gao and L. Chen, “Influence of right-angle prism tilt on azimuth laying accuracy,” *Acta Photon.* **31**, 117-119 (2002).
 17. J. Wang and J. Bai, “The measure of the right-angle prism Axis’s comparatively variety,” *Sci. Technol. Eng.* **18**, 2881-2886 (2006).